PCCP

PAPER

View Article Online
View Journal | View Issue

Check for updates

Cite this: *Phys. Chem. Chem. Phys.*, 2022, **24**, 9298

Geometrical picture of the electron–electron correlation at the large-*D* limit

Kumar J. B. Ghosh,[ab] Sabre Kais[b] and Dudley R. Herschbach *[c]

In electronic structure calculations, the correlation energy is defined as the difference between the mean field and the exact solution of the non relativistic Schrödinger equation. Such an error in the different calculations is not directly observable as there is no simple quantum mechanical operator, apart from correlation functions, that correspond to such quantity. Here, we use the dimensional scaling approach, in which the electrons are localized at the large-dimensional scaled space, to describe a geometric picture of the electronic correlation. Both, the mean field, and the exact solutions at the large-*D* limit have distinct geometries. Thus, the difference might be used to describe the correlation effect. Moreover, correlations can be also described and quantified by the entanglement between the electrons, which is a strong correlation without a classical analog. Entanglement is directly observable and it is one of the most striking properties of quantum mechanics and bounded by the area law for local gapped Hamiltonians of interacting many-body systems. This study opens up the possibility of presenting a geometrical picture of the electron–electron correlations and might give a bound on the correlation energy. The results at the large-*D* limit and at $D = 3$ indicate the feasibility of using the geometrical picture to get a bound on the electron–electron correlations.

Received 26th January 2022,
Accepted 29th March 2022

DOI: 10.1039/d2cp00438k

rsc.li/pccp

Published on 30 March 2022. Downloaded on 1/26/2026 11:56:33 PM.

1 Introduction

Dimensional scaling, as applied to electronic structure calculations, offers promising computational strategies and heuristic perspectives with physical insight of the electronic structure of atoms, molecules and extended systems.[1–4] Taking the spatial dimension of the physical space as a variable other than $D = 3$ can make a problem much simpler and then one can use perturbation theory or other techniques to obtain the results at $D = 3$. The *D*-scaling technique was used first in quantum chromodynamics[5] and then applied to the Helium atom.[2–4] In this approach, we solve the problem at the $D \to \infty$ limit and then add terms in powers of $\delta = 1/D$. Using different summation techniques[6] can obtain highly accurate results for $D = 3$. The dimensional scaling approaches were extended to *N*-electron atoms,[7] renormalization with $1/Z$ expansions,[8] random walks,[9,10] interpolation of hard sphere virial coefficients,[11] resonance states[12] and dynamics of many-body systems in external fields.[13,14] We refer the reader to the book "Dimensional scaling in chemical physics"[15] for more details of the approach and applications.

In computational physics and chemistry, the Hartree-Fock (HF) method[16] is a self-consistent field approximation to determine the wave function and the energy of a quantum many-body system in a stationary state. This method is based on the idea that we can approximately describe an interacting electronic system in terms of an effective single-particle model. Moreover, this simple approximation remains the starting point for more accurate post Hartree–Fock methods such as coupled clusters and configuration interactions.

The Hartree-Fock method assumes that the exact *N*-body wave function of the system can be approximated by a single Slater determinant of *N* spin-orbitals. In quantum chemistry calculations, the correlation energy is defined as the difference between the Hartree-Fock limit energy and the exact solution of the nonrelativistic Schrödinger equation.[17] Other measures of electron correlation also exist in the literature, for *e.g.* the statistical correlation coefficients.[18] Recently the Shannon entropy is also described as a measure of the correlation strength.[19,20] Electron correlations have wide implications on atomic, molecular,[21] and solid state physics.[22] Observing the correlation energy for large systems is one of the most challenging problems in quantum chemistry because there is no simple operator in quantum mechanics that its measurement gives the correlation energy. This leads to proposing the entanglement as an alternative measure of the electron correlation for atoms and molecules.[23] All the information needed for quantifying the entanglement is contained in the two-electron density matrix.

[a] *E.ON Digital Technology GmbH, 45131, Essen, Germany. E-mail: jb.ghosh@outlook.com*
[b] *Department of Chemistry and Physics, Purdue University, West Lafayette, IN, 47906, USA. E-mail: kais@purdue.edu*
[c] *Department of Chemistry and Chemical Biology, Harvard University, Cambridge, MA 02138, USA. E-mail: dherschbach@gmail.com*

This journal is © the Owner Societies 2022

Published on 30 March 2022. Downloaded on 1/26/2026 11:56:33 PM.

This measure is readily calculated by evaluating the von Neumann entropy of the one electron reduced density operator. As an example, one can see the calculation of the entanglement for He atom and H_2 molecule with different basis sets.[23] The advantage of this proposal is that entanglement is directly observable, and it is one of the most striking properties of quantum mechanics.

Entanglement is a quantum mechanical property that describes strong correlations between quantum mechanical particles that has no classical analog and has been studied extensively in the field of quantum information and quantum computing.[24–29] Moreover, scientists studied numerous properties of the entanglement entropy,[30–33] addressing many interesting topics of physics, for example black hole physics,[34–36] distribution of quantum correlations in quantum many-body systems in one dimension[30,37,38] and higher dimensions,[39–42] complexity of quantum many-body systems and their simulation,[43,44] and topological entanglement entropy.[45–49]

In this article we describe a geometric interpretation of correlation energy calculated at large-D limit and at three dimensions and establish a relation between the correlation energy and the area law of entanglement. In Section 2, we describe the area law of entanglement. In Sections 3 and 4, we describe the relation between the area difference and the correlation energy of the atomic/ionic systems and metallic hydrogen at the large-D limit. In Section 5, we consider the helium atom and the metallic hydrogen at $D = 3$, where the electrons are not localized unlike in the $D \to \infty$ limit. Finally, in Section 6, we make some concluding remarks. We adopt Hartree atomic units for our calculations.

2 Area law of entanglement

In classical physics, concepts of entropy quantify the amount of information that is lacking to identify the microstate of a physical system from all the possibilities compatible with the macrostate of the system. In quantum mechanics, we define the entanglement entropy or geometric entropy,[50–52] which arises because of a very fundamental property called entanglement. In quantum many-body systems, for a pure state $\rho = |\psi\rangle\langle\psi|$, the von Neumann entropy is a good measure of entanglement and defined as[50]

$$S(\rho) = -\mathrm{tr}[\rho \log_2 \rho] \tag{1}$$

Generally, a quantum state $|\psi\rangle$ of n-qubits (spin $\frac{1}{2}$) is represented as a vector in $(\mathbb{C}^2)^{\otimes n}$,

$$|\psi\rangle = \sum_{i_1,\ldots,i_n} C_{i_1,\ldots,i_n} |i_1,\ldots,i_n\rangle. \tag{2}$$

This is a very complex wave function with complex coefficients C_i, in Hilbert space of dimension $\mathbb{C}^{2^n}$. One way to find a possible efficient representation, is to examine a bipartite system with a local gapped Hamiltonian, summing over nearest neighbor interacting particles, as shown in Fig. 1.[53–57] The entanglement entropy between the interior state X and the exterior state X^c scales as the size of the boundary for every region X,

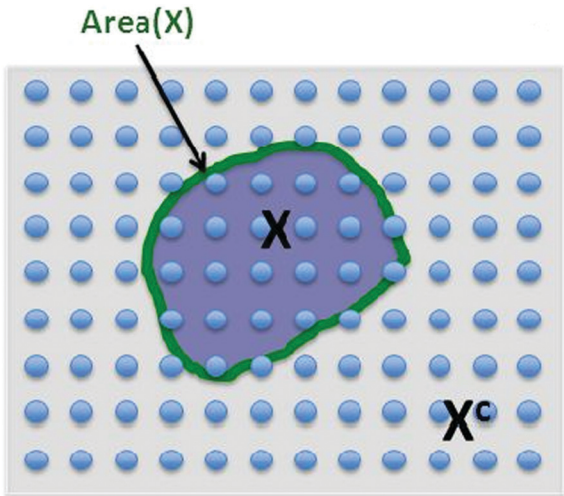

Fig. 1 The area law of the entanglement entropy: We have n-qubits (spin $\frac{1}{2}$ particles) in two-dimensional space interacting with local Hamiltonians (sum over nearest neighbor integrating particle) and the question is what is the entanglement between the interior shaded area X and the exterior system X^c. The conjecture of the area law is that the entanglement is bounded by the size of the boundary as shown above. The number of qubits in Fig. is for the demonstration purpose only (just a cartoon).

$$S(\mathrm{X}) \leq \text{constant} \times \mathrm{Area}(\mathrm{X}). \tag{3}$$

Recently, the area law of bounding the entanglement entropy of the ground state energy was examined for local integrating particles with large gapped energy spectrum.[53–57] It is shown that the ground state of a chain of d-dimensional spins with a boundary L and spectral gap δ is bounded by an area law

$$S_{1D}(L) = \exp(\mathcal{O}(\log(d)/\delta)) = \text{constant}, \tag{4}$$

where $\mathcal{O}(\ldots)$ is used to denote a bound up to a numeric constant of order unity. The area law for the entanglement entropy and ground state of local Hamiltonian was further extended to two dimensional lattice.[58–62] Here, we use the area law as a heuristic approach to guide us to discuss having a possible bound on the electronic correlation energy as one can obtain a well define geometrical picture of the localized electrons at the large-D limit, for both the mean field and the exact electronic structure.

3 Correlation energy and the surface area for atomic systems at the large-D limit

At the large-D limit, one can obtain a simple formula for the electronic structure of N-electron atoms.[7] At $D \to \infty$ limit, the electrons are localized in the scaled space with equidistant r_m from the nucleus and equiangular with respect to each other, which means that there is no shell structure. This simple geometrical picture holds for a wide variety of atoms and ions

Published on 30 March 2022. Downloaded on 1/26/2026 11:56:33 PM.

including all neutral atoms with $Z < 14$ and all positive ions with $N/Z \lesssim 0.936$.[7] In the Hartree–Fock limit all electrons are orthogonal to each other. The electronic energy $\varepsilon_\infty^{\mathrm{HF}}$ and distance from the nucleus $r_{\mathrm{m}}^{\mathrm{HF}}$ of an N-electron atom are described by the following formulas:

$$\varepsilon_\infty^{\mathrm{HF}} = -\frac{N}{2}\left[1 - 2^{3/2}(N-1)\lambda\right]^2, \tag{5}$$

$$r_{\mathrm{m}}^{\mathrm{HF}} = [1 - 2^{3/2}\,(N-1)\,\lambda]^{-1}, \tag{6}$$

with $\lambda = 1/Z$, where Z is the nuclear charge. For larger atoms the global minimum of the Hamiltonian H_∞ no longer has a maximal symmetry and the solutions display a kind of meta-shell structure, but one which is apparently unrelated to the normal three dimensional shell structure.[7]

After adding the inter-electronic correlation in the picture the electrons are no more orthogonal to one another. Therefore, the inter-electronic angle θ_∞ becomes slightly larger than $\pi/2$, although their equi-distance property from the nucleus ρ_∞ still holds. At $D \to \infty$ limit the relevant quantities can be calculated by the following formula:

The exact energy is given by

$$\varepsilon_\infty = -\frac{1}{2}\left(\frac{1-\xi}{1-\xi/N}\right)^3 (N - N\xi + \xi), \tag{7}$$

the inter-electronic angle

$$\theta_\infty = \arccos\left(\frac{\xi}{\xi - N}\right), \tag{8}$$

and the electronic distance

$$\rho_\infty = \left(\frac{1-\xi/N}{1-\xi}\right)^2 (N - N\xi + \xi), \tag{9}$$

where the parameter ξ is the smallest positive root obtained by solving the following quartic equation

$$8NZ^2\xi^2\,(2-\xi)^2 = (N-\xi)^3. \tag{10}$$

We solve the above sets of eqn (5) and (7) numerically and calculate the correlation energy at $D \to \infty$ limit which is defined by

$$\varepsilon_\infty^{\mathrm{Corr}} = |\varepsilon_\infty - \varepsilon_\infty^{\mathrm{HF}}|. \tag{11}$$

For example, from the above eqn (5)–(9), we obtain the following results for the helium-atom $r_{\mathrm{m}}^{\mathrm{HF}} = 1.214737$, $\varepsilon_\infty^{\mathrm{HF}} = -0.6776966$, $\rho_\infty = 1.213927$, $\theta_\infty = 1.663309$ rad, $\varepsilon_\infty = -0.68444228$, and $\varepsilon_\infty^{\mathrm{Corr}} = 0.0067456$.

Next, we draw the following geometrical pictures of the two localized electrons of the helium-atom at $D \to \infty$. We first construct a right angle triangle with two equal sides equal to $r_{\mathrm{m}}^{\mathrm{HF}}$ and another isosceles triangle with two equal sides equal to ρ_∞ and the inter-electronic angle θ_∞.

In Fig. 2, the nucleus is fixed at the point A. The points B and C describe the positions of the two electrons at HF-limit, whereas the points D and E describe the positions of the two electrons with correlation. At HF-limit $ABpAC$ however the correlation angle $\angle EAD > \pi/2$.

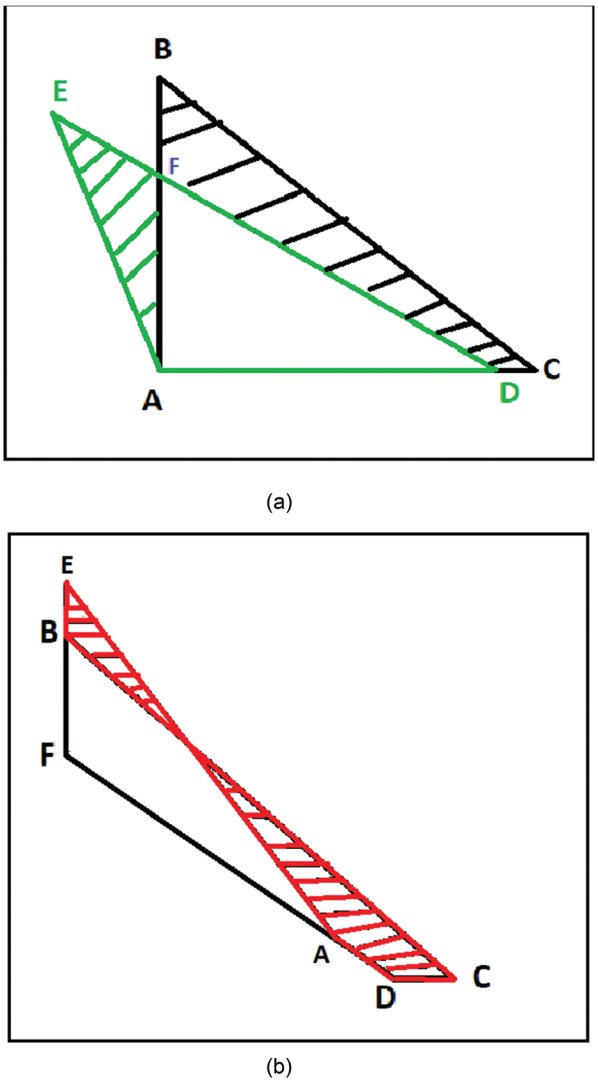

Fig. 2 The geometry of the localized electrons in a helium atom is described at large-D limit. Without inter-electronic correlation the electrons B and C are orthogonal with respect to the nucleus A. Whereas, with correlation the inter-electronic angle $\angle DAE$ becomes slightly larger than $\pi/2$. At the top panel (a), we draw the triangles formed by the two electrons and the nucleus with (ΔCAB) and without correlation (ΔDAE). At the bottom (b), the area difference between the two triangles is described by the striped red region.

The area of the isosceles triangle was calculated with the simple formula $\Delta ADE = \frac{1}{2}AE \times AD \times \sin(\angle EAD)$. Then we calculate the magnitude of the area difference (Δarea) between the ΔABC and ΔADE for the helium atom Δarea = 0.00413417. In Fig. 2 we show the area difference as the difference between the stripped areas.

For three-electron atoms we construct the three triangles ΔABC, ΔACD, and ΔADB (see Fig. 3). The point A is the position of nucleus and the points B, C, D are three localized electronic positions. The sides $AD = AC = AB$. At HF-limit, the

 This journal is © the Owner Societies 2022

Published on 30 March 2022. Downloaded on 1/26/2026 11:56:33 PM.

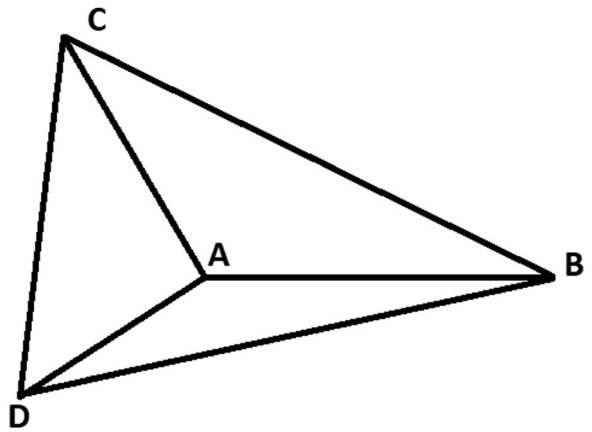

Fig. 3 Geometry of a three-electron atom at $D \to \infty$ limit. The point A is the position of nucleus and the points B, C, D are three localized electronic positions.

angles $\angle BAC = \angle CAD = \angle BAD = \pi/2$, whereas, with correlation $\angle BAC = \angle CAD = \angle BAD > \pi/2$.

As an extension of the above, we construct N-triangles for N-electron atoms and compute the total areas for both HF and with inter-electronic correlation. Then we compute the area difference for N-triangles between HF and electronic-correlation.

In Fig. 4, we describe the area difference which is computed from the N-triangles of the N-electron atom.

We compute the correlation energies for N-electron atoms, using eqn (5) and (7), and plot this in Fig. 5 along with the area differences obtained above.

We also compute the inverse of the electronic correlation energies and the inverse of the area difference obtained from the above prescription and plot these in Fig. 6.

In Fig. 5 and 6, we see that the area difference is a close estimate to the correlation energy at the large-D limit. On the other hand, it was shown by Loeser *et al.*[7] that the correlation energy at $D = 3$ is a good approximation to the correlation energy at $D \to \infty$. Therefore the correlation energy is bounded by the area difference of the electronic triangles between the HF-limit and with correlation at large-D limit. We plot the known accurate correlation energies at $D = 3$[63–66] and with the correlation energies obtained at $D = \infty$.

In Fig. 7, we see that the correlation energies at $D = 3$ are bounded by the corresponding area differences at $D \to \infty$ limit, with the only exception for $N = 2$.

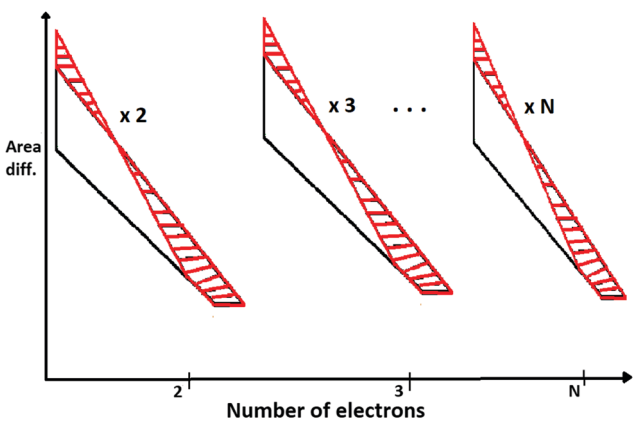

Fig. 4 The area differences calculated for N-electron atoms at $D \to \infty$ limit. Because of special symmetry at the large-D limit, area difference per number of electrons is the same.

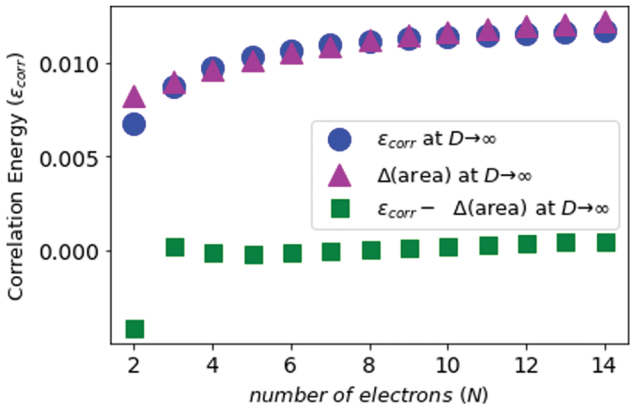

Fig. 5 The electronic correlation energies (in Z^2 Hartree) for neutral atoms from $N = 2$ to $N = 14$ in blue, and the area difference in purple. The green points are the difference between the above two results.

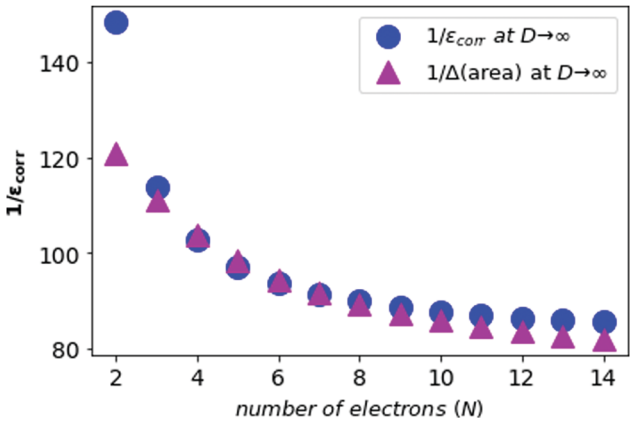

Fig. 6 The inverse of the electronic correlation energies for neutral atoms from $N = 2$ to $N = 14$ in blue, and the inverse of area difference in purple.

4 Electron correlation and the surface area for metallic hydrogen at the large-D limit

In 1935, Wigner and Huntington predicted the metallization of hydrogen,[67] a phase of hydrogen that behaves like an electrical conductor. Ever since this has been a major quest for condensed matter physics, pursuing theory[68–72] and extreme high-pressure experiments.[73–78] Dimensional scaling and interpolation as applied to metallic hydrogen was investigated in articles.[68,79] With appropriate scaling, energies will be in units of $4/(D-1)^2$ Hartrees, and distances in units of $D\,(D-1)/6$ Bohr radii. we

Published on 30 March 2022. Downloaded on 1/26/2026 11:56:33 PM.

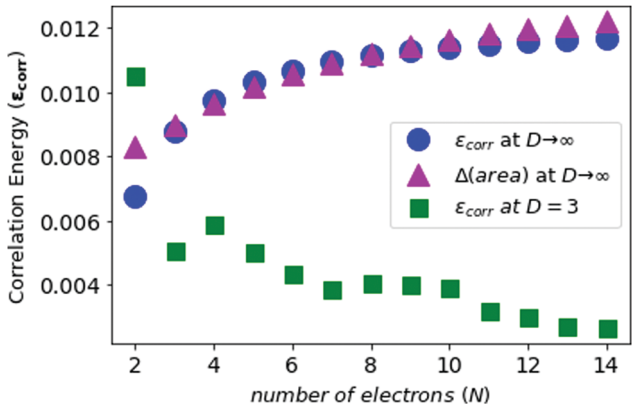

Fig. 7 The electronic correlation energies for neutral atoms from N = 2 to N = 14 in blue, the area differences in purple, and correlation energies at D = 3 in green. Note that the energies are represented in the Z^2 Hartree.

consider the lattice to be simple cubic (SC). With scaling and simplifications, the Hartree–Fock one-electron Hamiltonian in the $D \to \infty$ limit in a lattice of hydrogen atoms with clamped nuclei can be written as:[68]

$$\mathscr{H} = \frac{9}{8\rho^2} - \frac{3}{2\rho} + W(\rho, R), \tag{12}$$

where ρ is the scaled electron-nucleus distance, R is the nuclear position and

$$W(\rho,R) = \frac{3}{4}\sum_{l,m,n\in\mathscr{L}'} \frac{1}{\sqrt{\sigma^2R^2}} - \frac{2}{\sqrt{\sigma^2R^2+\rho^2}} + \frac{1}{\sqrt{\sigma^2R^2+2\rho^2}}, \tag{13}$$

with integers (l, m, n) are given by the lattice symmetry

$$\sigma^2 = l^2 + m^2 + n^2. \tag{14}$$

For any specified lattice type and scaled lattice constant R, the minimum of eqn (12) with respect to ρ gives the energy per electron. The whole lattice is three-dimensional, noted $\mathscr{L}'$ minus the one site (0,0,0). The single variable ρ is the orbit radius and R is the lattice spacing.

We introduce the inter-electronic correlation at $D \to \infty$ limit by opening up the dihedral angles from their Hartree–Fock values of exactly $\pi/2$ rad. The dihedral angles in the correlated solution is determined by two effects, namely, the centrifugal effects, favoring $\pi/2$ rad, and interelectron repulsions, favoring π rad. Although the final effect turns out to be the angles very close to $\pi/2$ rad. For the calculation purpose we assume the inter-electronic correlation is up to third nearest neighbor, which is a very legitimate assumption. We assume the lattice structure to be simple cubic (SC).

At $D \to \infty$ limit, the Hamiltonian with inter-electronic correlation can be written as:[68]

$$\mathscr{H}_{\text{corr}} = \mathscr{H}_{\text{HF}} + \frac{9}{8\rho^2}\left(\left(\frac{\Gamma'}{\Gamma}\right)^{(3)} - 1\right) + \frac{3}{2}W_{\Delta}^{(3)}, \tag{15}$$

where

$$W_{\Delta}^{(3)} = 6\Delta W(\rho, R, \gamma_{100}) + 12\Delta W(\rho, \sqrt{2}R, \gamma_{110}) + 8\Delta W(\rho, \sqrt{3}R, \gamma_{111}), \tag{16}$$

with

$$\Delta W(\rho, \sigma R, \gamma_{lmn}) = \frac{1}{2}\left(\frac{1}{\sqrt{\sigma^2R^2 + 2\rho^2(1-\gamma_{lmn})}} - \frac{1}{\sqrt{\sigma^2R^2+2\rho^2}}\right). \tag{17}$$

The $\mathscr{H}_{\text{HF}}$ is the Hamiltonian in Hartree–Fock approximation defined in eqn (12). The quantity $\gamma_{lmn} = \cos\theta_{lmn}$, with θ_{lmn} are the dihedral angles which are very close to $\pi/2$. The Gramian ratio $\left(\frac{\Gamma'}{\Gamma}\right)^{(3)}$ is defined as[68]

$$\left(\frac{\Gamma'}{\Gamma}\right)^{(3)} \simeq 1 + 6{\gamma_{100}}^2 + 12{\gamma_{110}}^2 + 8{\gamma_{111}}^2 + (\text{higher order terms in } \gamma). \tag{18}$$

We optimize the above Hamiltonian (15) with respect to the parameters γ_{100},γ_{110},γ_{111}, keeping the values of ρ and R from the HF-Hamiltonian.[79]

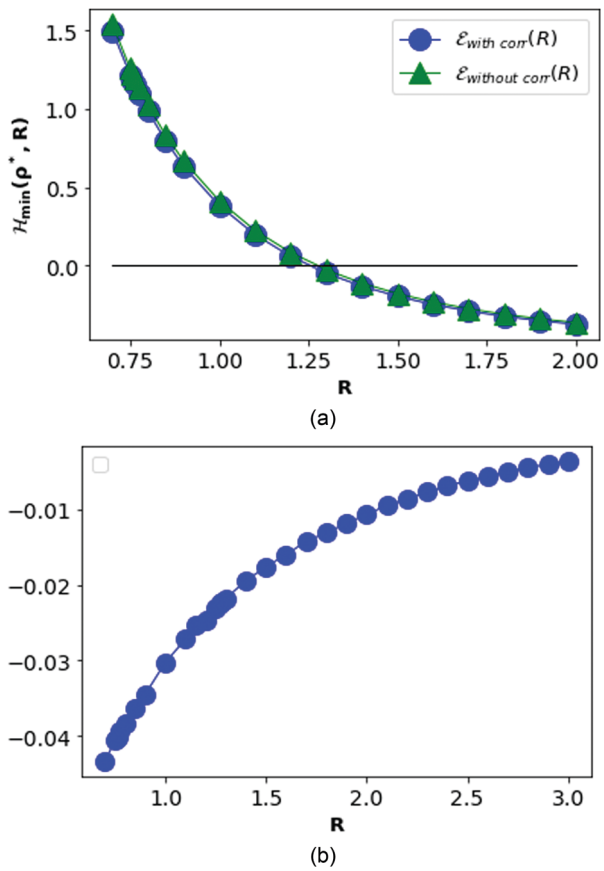

Fig. 8 At the top panel (a), we plot the energy obtained at $D \to \infty$ with inter-electronic correlation in blue, compared with the HF energy as a function of R in green. At the bottom (b), we plot the correlation energy as a function of R.

 This journal is © the Owner Societies 2022

Published on 30 March 2022. Downloaded on 1/26/2026 11:56:33 PM.

In Fig. 8, we plot the minimum values of the Hamiltonian (15) at $D \to \infty$ limit as function of R and compare with the values obtained from the HF-Hamiltonian. We also plot the correlation energies $\mathscr{E}_{\text{corr}} = \mathscr{H}_{\text{corr}} - \mathscr{H}_{\text{HF}}$ as a function of R. In the left hand side of Fig. 8, we see that the ground state energy becomes positive for $R < 1.28$, therefore makes the system unstable. Therefore, $R > 1.28$ can be think of a physically stable region for metallic hydrogen at $D \to \infty$ limit.

In the simple cubic lattice at $D \to \infty$ limit, the electrons also forms a cubic structure. With each reference electron there are 6 nearest neighbors at a distance R, 12 second nearest neighbors at a distance $\sqrt{2}R$, 8 third nearest neighbors at a distance $\sqrt{3}R$ and so on. At HF-limit the nearest neighbours (N_{1i} for $i = 1, 2, \ldots 6$) are orthogonal to each other with respect to the reference electron (O). For correlation the dihedral angles between the electrons becomes slightly greater than 90°. The following figure describes a cross section of a MH in SC lattice with reference electron O. In HF limit we consider 6 square surfaces for 6 neighbouring electrons at a distance R, 12 square surfaces for 12 neighbouring electrons at a distance $\sqrt{2}R$, and 8 square surfaces for 8 neighboring electrons at a distance $\sqrt{3}R$. Whereas, with inter-electronic correlation each square becomes a rhombus.

In Fig. 9, we plot the area difference due to the electronic correlation. The area difference between the square and the rhombus formed by each nearest neighbor is equal to $R^2(1 - \cos\theta)$, where $\theta = \gamma_{100} - 90°$ is the angle deviation from 90° due to correlation effect. The area difference for each next nearest neighbor is equal to $2R^2(1 - \cos\theta_2)$, with $\theta_2 = \gamma_{110} - 90°$, and so on. The total area difference due to the correlation up to the third nearest neighbor is given by:

$$\Delta\text{area} = 6R^2(1 - \cos(\gamma_{100} - 90°)) + 24R^2(1 - \cos(\gamma_{110} - 90°)) + 24R^2(1 - \cos(\gamma_{111} - 90°)). \tag{19}$$

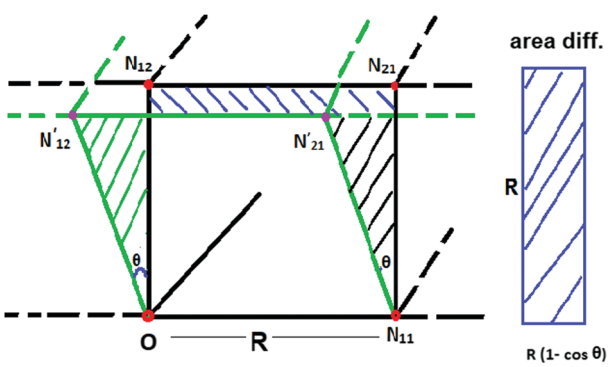

Fig. 9 The area difference for a single cell formed by each nearest neighbor. N_{11}, N_{12} are the positions of the two nearest electrons in HF representation w.r.t. the reference electron O; whereas the primed ones for *e.g.*, N'_{12}, N'_{21} are the relative positions of the first and second nearest neighbor electrons respectively due to the inter electronic correlation. In the right, the area difference is represented by the blue stripped region.

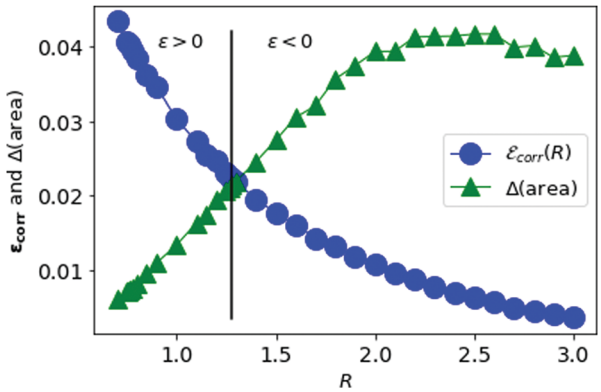

Fig. 10 The correlation energy per electron in metallic hydrogen at $D \to \infty$ as a function of R in blue and the area difference in green.

We vary the lattice parameter R and calculate the area difference for each value of R. In Fig. 10, we plot the correlation energy per electron for metallic hydrogen in SC lattice at large-D limit and the area difference described above as a function of the lattice parameter R.

In Fig. 10, we see that the correlation energy per electron is bounded by the area difference in the physically stable region (*i.e.* total ground state energy $\varepsilon > 0$).

The correlation energy per electron (in Rydberg unit) in metallic hydrogen at $D = 3$ was calculated by Neece *et al.*[80,81]

$$\varepsilon_{\text{corr}} = -0.1303 + 0.0495\ln(r_s). \tag{20}$$

In the above eqn (20), the lattice constant R is related to r_s, the standard solid state parameter, defined as the radius of a sphere (in a_0 Bohr units) in which contains on average one electron. For the SC lattice,

$$\frac{4}{3}\pi r_s^3 = R^3. \tag{21}$$

In Fig. 11, we plot the correlation energy of each electron in metallic hydrogen as a function of R at $D = 3$ and compare with the $D = \infty$ result.

In Fig. 11, we see that the correlation energy per electron ($\varepsilon_{\text{corr}}$) at $D \to \infty$ is bounded by $\varepsilon_{\text{corr}}$ at $D = 3$. Although at $D = 3$, there is no concept of the dihedral angles between electrons as the electrons are not localized. We shall calculate the corresponding area difference for metallic hydrogen at three dimensions in the next section.

5 Correlation energy and the surface area difference in the three-dimension

In the previous sections, we established that the correlation energies are bounded by the area differences for N-electron atoms and also for metallic hydrogen at the large-D limit. In three dimensions, the picture is different, because at $D = 3$ the electrons are not localized compared to the $D \to \infty$ limit. To establish the validity of the area law and correlation energy, we consider the helium atom in three-dimensions. The two 1s

Published on 30 March 2022. Downloaded on 1/26/2026 11:56:33 PM.

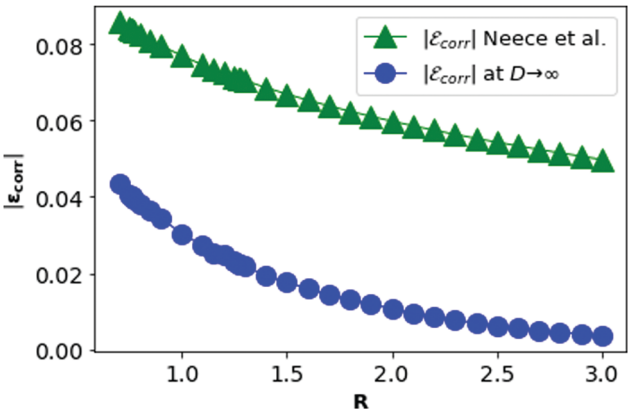

Fig. 11 The correlation energy per electron in metallic hydrogen at $D \to \infty$ as a function of R in blue and at $D = 3$ in green.

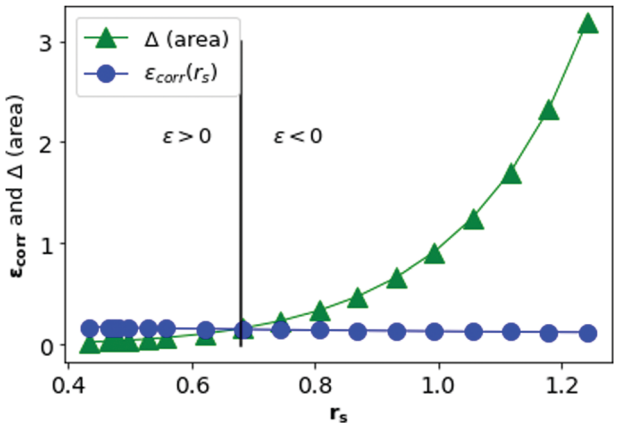

Fig. 13 Δ(area) and $\varepsilon_{\text{corr}}$ are plotted as a function of r_s in blue and green respectively.

electrons in the helium atom at 3D are in spherical orbitals with an average electronic radius $\langle r \rangle$. The average radius changes from $\langle r_{\text{HF}} \rangle$ (in HF approximation) to $\langle r_{\text{exact}} \rangle$ (with inter-electronic correlation). The area difference is the difference between the two spherical surfaces with radii $\langle r_{\text{HF}} \rangle$ and $\langle r_{\text{exact}} \rangle$ respectively.

In the Hartree–Fock approximation, the average electronic radius[82,83] is given by $\langle r_{\text{HF}} \rangle = 0.92724$ a.u. On the other hand, with inter-electronic correlation, a very accurate value of $\langle r_{\text{exact}} \rangle = 0.92947$ was computed by Thakkar *et al.*[84]

The surface area difference between the two spherical orbitals is calculated as

$$\Delta\text{area} = 4\pi\,(r_{\text{HF}}{}^2 - r_{\text{exact}}{}^2) = 0.0520. \tag{22}$$

Whereas, the correlation energy of the helium atom[63,64,85] in atomic unit is given by $|\varepsilon_{\text{corr}}| = 0.04204$. Therefore, the correlation energy is bounded by the area difference in three-dimensions also.

From DFT calculations the ground state energy (in Rydberg unit) per electron in metallic hydrogen in simple cubic lattice at $D = 3$ is expressed as[86]

$$\varepsilon(r_s) = \frac{2.21}{r_s{}^2} - \frac{2.80604}{r_s} - 0.13993 - 0.11679\ln(r_s), \tag{23}$$

where r_s is the average atomic radius of each hydrogen atom in MH.

In Fig. 12, we see that the ground state energy becomes positive for $r_s < 0.68$, therefore makes the system unstable. Therefore, $r_s > 0.68$ can be think of a physically stable region for metallic hydrogen at $D = 3$.

Now, if we introduce inter-electronic correlation, the average atomic radius in metallic hydrogen will change, *i.e.* the r_s will change. Therefore, we can think of the correlation energy as the change in the ground state energy due to a change in the atomic radius r_s, *i.e.*

$$\varepsilon_{\text{corr}}(r_s) = \frac{d\varepsilon(r_s)}{dr_s}\Delta r_s = \varepsilon'(r_s)\Delta r_s, \tag{24}$$

where $\varepsilon_{\text{corr}}$ (r_s) is defined in eqn (20) and ε (r_s) is defined in eqn (23). On the other hand, the change in the area per atom in metallic hydrogen is given as

$$\Delta(\text{area})(r_s) = \Delta(4\pi r_s{}^2) = 8\pi r_s\Delta r_s = 8\pi r_s\varepsilon_{\text{corr}}\,(r_s)/\varepsilon'\,(r_s). \tag{25}$$

In Fig. 13, we plot the Δ(area) and $\varepsilon_{\text{corr}}$ as a function of r_s. We see that the correlation energy per electron in MH is bounded by the area difference in the physically stable region (*i.e.* total ground state energy $\varepsilon > 0$) in three-dimension also.

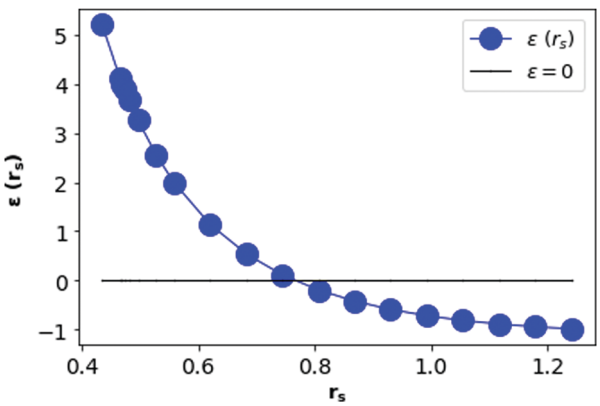

Fig. 12 Total ground state energy (in Rydberg unit) per electron in metallic hydrogen at $D = 3$ as a function of r_s.

6 Conclusion

Understanding quantum correlation in many-body states of matter, a feature ubiquitous in different problems of physics and chemistry, has gained renewed prominence in recent years. Experimentally, different protocols have been proposed to directly extract spatial correlation functions in phases like in the Mott regime of a Hubbard Hamiltonian[87,88] due to single-site resolution and selective spin removal technique afforded by quantum-gas microscopy in platforms like ultracold-atomic

 This journal is © the Owner Societies 2022

Published on 30 March 2022. Downloaded on 1/26/2026 11:56:33 PM.

lattices. Such techniques have also been used to study response of magnetic field on an spin-imbalanced 2D lattice of fermions wherein there is a competition to maintain the anti-ferromagnetic checkerboard pattern and alignment with the externally applied field leading to canted lattices.[89] Even dynamical correlation from retarded Green's function can be obtained experimentally using Ramsey interferometry as illustrated in ref. 90 and in quantum simulator of over 100 trapped ions in a Penning trap through carefully designed echo sequences as illustrated in ref. 91.

On the other hand, for atomic and molecular systems as studied in traditional electronic structure as well as in this report, different theoretical measures have also been proposed to quantify the extent of deviation from the mean-field Hartree–Fock state like von Neumann entropy with the eigenvalues of the one-particle reduced density matrix (1-RDM)[92] or the Cumulant Expansion of the two-particle reduced density matrix (2-RDM).[93,94] The latter in particular affords many useful characterization including its relationship to eigenvalues of the 2-RDM itself and to long-range order,[95] its relationship to von Neumann entropy[96] and its relationship to various orders of cluster amplitudes for a Couple-Cluster (CC) based wavefunction ansatz.[97] It has been successfully used to probe electronic correlation in various problems[98–100] and very recently in capturing signatures of van der Waals interaction.[101]

Akin to the latter, in this paper we propose another metric with a simple geometrical insight which can be theoretically used to detect deviation from mean-field behavior and relate the said quantity through an area law to the correlation energy. This is timely as recently various studies[23,102–104] have shown that the entanglement, a quantum observable, can be used in quantifying the correlation energy in atomic and molecular systems. Moreover, a number of studies have shown that the ground state of a local Hamiltonian satisfies an area law and is directly related to the entanglement entropy.[53–62] On the other hand, the correlation energy of a system is the difference between the ground state energies in the HF and the accurate calculations. Therefore, the correlation energy is expected be bounded by the area difference when we go beyond the Hartree–Fock approximation to an exact representation. From Fig. 5, we see that the area difference for atomic/ionic systems at large-D limit is a close estimate to the correlation energy of the system. In fact at large-D limit $\varepsilon_{\text{corr}} \simeq \Delta(\text{area})$. In three-dimension, for helium atom, the area difference (0.0520) is close to the correlation energy 0.0420. From eqn (25), the average correlation energy of metallic hydrogen in three dimensions can be described as

$$\varepsilon_{\text{corr}}(r_s) = \alpha\Delta(\text{area}), \tag{26}$$

with $\alpha = \varepsilon'(r_s)/(8\pi r_s)$. Combining the above results described in the previous sections we can write an area law for correlation energy as follows

$$\varepsilon_{\text{corr}} \leq C\Delta(\text{area}), \tag{27}$$

with some proportionality constant C, which looks similar to eqn (3), the area law for entanglement entropy.

In summary, we have shown that the correlation energy might be bounded by an area law which is a close resemblance of the area law conjecture of entanglement entropy. The advantage of this proposal is that we establish a relation between the correlation energy, which is an indirect measure, and the entanglement, which is directly observable, and it is one of the most striking properties of quantum mechanics. Examining the electron correlation in terms of geometry changes between mean field and exact solution might open a new way to observe the correlation effect.

Conflicts of interest

There are no conflicts to declare.

Acknowledgements

We would like to thank Dr Manas Sajjan and Dr Andrew Hu for useful discussions and their comments on the manuscript. S. K. would like to acknowledge funding by the U.S. Department of Energy (Office of Basic Energy Sciences) under Award No. DE-SC0019215.

References

1 D. Herrick and F. Stillinger, *Phys. Rev. A: At., Mol., Opt. Phys.*, 1975, **11**, 42–53.
2 L. Mlodinow and N. Papanicolaou, *Ann. Phys.*, 1980, **128**, 314–334.
3 L. Yaffe, *Rev. Mod. Phys.*, 1982, **54**, 407.
4 D. Herschbach, *J. Chem. Phys.*, 1986, **84**, 838–851.
5 E. Witten, *Phys. Today*, 1980, **33**, 38–43.
6 D. Goodson, M. López-Cabrera, D. Herschbach and J. Morgan III, *J. Chem. Phys.*, 1992, **97**, 8481–8496.
7 Z. Zhen and J. Loeser, in *Large-D Limit for N-Electron Atoms*, ed. D. Herschbach, J. Avery and O. Goscinski, Springer Netherlands, Dordrecht, 1993, pp. 83–114.
8 S. Kais and D. Herschbach, *J. Chem. Phys.*, 1994, **100**, 4367–4376.
9 J. Rudnick and G. Gaspari, *Science*, 1987, **237**, 384–389.
10 K. J. B. Ghosh, S. Kais and D. R. Herschbach, *J. Phys. Chem. A*, 2021, **125**, 7581–7587.
11 J. Loeser, Z. Zhen, S. Kais and D. Herschbach, *J. Chem. Phys.*, 1991, **95**, 4525–4544.
12 S. Kais and D. Herschbach, *J. Chem. Phys.*, 1993, **98**, 3990–3998.
13 Q. Wei, S. Kais and D. Herschbach, *J. Chem. Phys.*, 2008, **129**, 214110.
14 Q. Wei, S. Kais and D. Herschbach, *J. Chem. Phys.*, 2007, **127**, 094301.
15 D. R. Herschbach, J. S. Avery and O. Goscinski, *Dimensional scaling in chemical physics*, Springer Science & Business Media, 2012.
16 J. C. Slater, *Phys. Rev.*, 1951, **81**, 385.
17 P. O. Löwdin, *Adv. Chem. Phys.*, 1958, 207–322.

Published on 30 March 2022. Downloaded on 1/26/2026 11:56:33 PM.

18 W. Kutzelnigg, G. Del Re and G. Berthier, *Phys. Rev.*, 1968, **172**, 49.
19 N. L. Guevara, R. P. Sagar and R. O. Esquivel, *Phys. Rev. A*, 2003, **67**, 012507.
20 Q. Shi and S. Kais, *J. Chem. Phys.*, 2004, **121**, 5611–5617.
21 S. Wilson, *Electron correlation in molecules*, Clarendon Press, Oxford, 1984.
22 N. H. March, *Electron Correlations in the Solid State*, World Scientific, 1999.
23 Z. Huang and S. Kais, *Chem. Phys. Lett.*, 2005, **413**, 1–5.
24 C. H. Bennett and D. P. DiVincenzo, *Nature*, 2000, **404**, 247–255.
25 C. Macchiavello, G. M. Palma and A. Zeilinger, *Quantum Computation and Quantum Information Theory*, World Scientific, 2000.
26 M. Nielsen and I. Chuang, *Quantum Computation and Quantum Information: 10th Anniversary Edition*, Cambridge University Press, USA, 10th edn, 2011.
27 J. Gruska *et al.*, *Quantum computing*, McGraw-Hill, London, 1999, vol. 2005.
28 E. Schrödinger, *Naturwissenschaften*, 1935, **23**, 823–828.
29 D. Bruß, *J. Math. Phys.*, 2002, **43**, 4237–4251.
30 K. Audenaert, J. Eisert, M. B. Plenio and R. F. Werner, *Phys. Rev. A: At., Mol., Opt. Phys.*, 2002, **66**, 042327.
31 T. J. Osborne and M. A. Nielsen, *Phys. Rev. A: At., Mol., Opt. Phys.*, 2002, **66**, 032110.
32 A. Osterloh, L. Amico, G. Falci and R. Fazio, *Nature*, 2002, **416**, 608–610.
33 G. Vidal, J. I. Latorre, E. Rico and A. Kitaev, *Phys. Rev. Lett.*, 2003, **90**, 227902.
34 J. D. Bekenstein, *JACOB BEKENSTEIN: The Conservative Revolutionary*, World Scientific, 2020, pp. 307–320.
35 L. Bombelli, R. K. Koul, J. Lee and R. D. Sorkin, *Phys. Rev. D*, 1986, **34**, 373.
36 M. Srednicki, *Phys. Rev. Lett.*, 1993, **71**, 666.
37 L. Amico, R. Fazio, A. Osterloh and V. Vedral, *Rev. Mod. Phys.*, 2008, **80**, 517.
38 T. Barthel, S. Dusuel and J. Vidal, *Phys. Rev. Lett.*, 2006, **97**, 220402.
39 S. Bravyi, M. B. Hastings and F. Verstraete, *Phys. Rev. Lett.*, 2006, **97**, 050401.
40 M. Cramer and J. Eisert, *New J. Phys.*, 2006, **8**, 71.
41 M. Cramer, J. Eisert, M. B. Plenio and J. Dreissig, *Phys. Rev. A: At., Mol., Opt. Phys.*, 2006, **73**, 012309.
42 M. B. Plenio, J. Eisert, J. Dreissig and M. Cramer, *Phys. Rev. Lett.*, 2005, **94**, 060503.
43 U. Schollwöck, *Rev. Mod. Phys.*, 2005, **77**, 259.
44 S. R. White, *Phys. Rev. Lett.*, 1992, **69**, 2863.
45 Z. Nussinov and G. Ortiz, *Ann. Phys.*, 2009, **324**, 977–1057.
46 X. G. Wen, *Phys. Rev. B: Condens. Matter Mater. Phys.*, 1989, **40**, 7387.
47 E. Witten, *Commun. Math. Phys.*, 1989, **121**, 351–399.
48 M. Haque, O. Zozulya and K. Schoutens, *Phys. Rev. Lett.*, 2007, **98**, 060401.
49 A. Kitaev and J. Preskill, *Phys. Rev. Lett.*, 2006, **96**, 110404.
50 J. Eisert, M. Cramer and M. B. Plenio, *Rev. Mod. Phys.*, 2010, **82**, 277.
51 R. Horodecki, P. Horodecki, M. Horodecki and K. Horodecki, *Rev. Mod. Phys.*, 2009, **81**, 865.
52 M. B. Plenio and S. S. Virmani, *Quantum Inf. Coherence*, 2014, 173–209.
53 M. B. Hastings, *Journal of statistical mechanics: theory and experiment*, 2007, **2007**, P08024.
54 M. B. Hastings, *Phys. Rev. B: Condens. Matter Mater. Phys.*, 2007, **76**, 035114.
55 I. Arad, A. Kitaev, Z. Landau and U. Vazirani, *arXiv preprint arXiv*, 2013, **1301**, 1162.
56 F. G. S. L. Brandão and M. Horodecki, *Nat. Phys.*, 2013, **9**, 721–726.
57 Z. Landau, U. Vazirani and T. Vidick, arXiv preprint arXiv:1307.5143.
58 M. M. Wolf, F. Verstraete, M. B. Hastings and J. I. Cirac, *Phys. Rev. Lett.*, 2008, **100**, 070502.
59 L. Masanes, *Phys. Rev. A: At., Mol., Opt. Phys.*, 2009, **80**, 052104.
60 N. de Beaudrap, T. J. Osborne and J. Eisert, *New J. Phys.*, 2010, **12**, 095007.
61 S. Michalakis, arXiv preprint arXiv:1206.6900, 2012.
62 A. Anshu, I. Arad and D. Gosset, arXiv preprint arXiv:2103.02492, 2021.
63 E. R. Davidson, S. A. Hagstrom, S. J. Chakravorty, V. M. Umar and C. F. Fischer, *Phys. Rev. A: At., Mol., Opt. Phys.*, 1991, **44**, 7071.
64 A. Veillard and E. Clementi, *J. Chem. Phys.*, 1968, **49**, 2415–2421.
65 D. Herschbach, J. Loeser and W. Virgo, *J. Phys. Chem. A*, 2017, **121**, 6336–6340.
66 S. Kais, S. Sung and D. Herschbach, *Int. J. Quantum Chem.*, 1994, **49**, 657–674.
67 E. Wigner and H. B. Huntington, *J. Chem. Phys.*, 1935, **3**, 764–770.
68 J. G. Loeser, *Large-D Limit for Metallic Hydrogen, Dimensional Scaling in Chemical Physics*, *Springer*, 1993, pp. 389–427.
69 H. K. Mao and R. J. Hemley, *Rev. Mod. Phys.*, 1994, **66**, 671.
70 C. S. Zha, Z. Liu and R. J. Hemley, *Phys. Rev. Lett.*, 2012, **108**, 146402.
71 R. P. Dias and I. F. Silvera, *Science*, 2017, **355**, 715–718.
72 J. McMinis, R. C. Clay III, D. Lee and M. A. Morales, *Phys. Rev. Lett.*, 2015, **114**, 105305.
73 R. J. Hemley and H. K. Mao, *Phys. Rev. Lett.*, 1988, **61**, 857.
74 R. J. Hemley, M. Hanfland and H. K. Mao, *Nature*, 1991, **350**, 488–491.
75 R. J. Hemley, H. K. Mao, A. F. Goncharov, M. Hanfland and V. Struzhkin, *Phys. Rev. Lett.*, 1996, **76**, 1667.
76 M. Zaghoo, A. Salamat and I. F. Silvera, *Phys. Rev. B*, 2016, **93**, 155128.
77 I. F. Silvera and R. Dias, *J. Phys.: Condens. Matter*, 2018, **30**, 254003.
78 P. Loubeyre, F. Occelli and P. Dumas, *Nature*, 2020, **577**, 631–635.
79 K. J. B. Ghosh, S. Kais and D. R. Herschbach, *Phys. Chem. Chem. Phys.*, 2021, **23**, 7841–7848.

 This journal is © the Owner Societies 2022

Published on 30 March 2022. Downloaded on 1/26/2026 11:56:33 PM.

80 G. Neece, F. Rogers and W. Hoover, *J. Comput. Phys.*, 1971, **7**, 621–636.
81 M. Ross and C. Shishkevish, *Molecular and metallic hydrogen*, Tech. Rep. RAND CORP SANTA MONICA CA, 1977.
82 J. B. Mann, *Technical Report, Los Alamos Scientific Laboratory*, 1968.
83 R. J. Boyd, *Can. J. Phys.*, 1977, **55**, 452–455.
84 A. J. Thakkar and V. H. Smith, *Phys. Rev. A: At., Mol., Opt. Phys.*, 1977, **15**, 1–15.
85 L. G. Jiao, L. R. Zan, L. Zhu and Y. K. Ho, *Comput. Theor. Chem.*, 2018, **1135**, 1–5.
86 B. I. Min, H. J. F. Jansen and A. J. Freeman, *Phys. Rev. B: Condens. Matter Mater. Phys.*, 1984, **30**, 5076–5083.
87 M. F. Parsons, A. Mazurenko, C. S. Chiu, G. Ji, D. Greif and M. Greiner, *Science*, 2016, **353**, 1253–1256.
88 A. Mazurenko, C. S. Chiu, G. Ji, M. F. Parsons, M. Kanász-Nagy, R. R. Schmidt, F. Grusdt, E. A. Demler, D. Greif and M. Greiner, *Nature*, 2017, **545**, 462–466.
89 P. T. Brown, D. Mitra, E. Guardado-Sanchez, P. Schauß, S. S. Kondov, E. Khatami, T. Paiva, N. Trivedi, D. A. Huse and W. S. Bakr, *Science*, 2017, **357**, 1385–1388.
90 M. J. Knap, A. Kantian, T. Giamarchi, I. Bloch, M. D. Lukin and E. A. Demler, *Phys. Rev. Lett.*, 2013, **111**(14), 147205.
91 M. Garttner, J. G. Bohnet, A. Safavi-Naini, M. L. Wall, J. J. Bollinger and A. M. Rey, *Nat. Phys.*, 2017, **13**, 781–786.
92 K. M. Pelzer, L. Greenman, G. Gidofalvi and D. A. Mazziotti, *J. Phys. Chem. A*, 2011, **115**(22), 5632–5640.
93 W. Kutzelnigg and D. Mukherjee, *J. Chem. Phys.*, 1999, **110**, 2800–2809.
94 D. A. Mazziotti, in *Cumulants and the Contracted Schrödinger Equation*, ed. J. Cioslowski, Springer US, Boston, MA, 2000, pp. 139–163.
95 A. Raeber and D. A. Mazziotti, *Phys. Rev. A: At., Mol., Opt. Phys.*, 2015, **92**, 052502.
96 M. Sajjan, K. Head-Marsden and D. A. Mazziotti, *Phys. Rev. A*, 2018, **97**, 062502.
97 L. Kong and E. F. Valeev, *J. Chem. Phys.*, 2011, **134**, 214109.
98 T. Juhasz and D. A. Mazziotti, *J. Chem. Phys.*, 2006, **125**, 174105.
99 J. W. Hollett and P.-F. Loos, *J. Chem. Phys.*, 2020, **152**, 014101.
100 D. R. Alcoba, R. C. Bochicchio, L. Lain and A. Torre, *J. Chem. Phys.*, 2010, **133**, 144104.
101 O. Werba, A. Raeber, K. Head-Marsden and D. A. Mazziotti, *Phys. Chem. Chem. Phys.*, 2019, **21**, 23900–23905.
102 L. Martina, G. Ruggeri and G. Soliani, *Int. J. Quantum Inf.*, 2011, **9**, 843–862.
103 M. R. Dowling, A. C. Doherty and S. D. Bartlett, *Phys. Rev. A: At., Mol., Opt. Phys.*, 2004, **70**, 062113.
104 A. Mohajeri and M. Alipour, *Int. J. Quant. Inf.*, 2009, **7**, 801–809.